Polymer 51 (2010) 1088–1099

Contents lists available at ScienceDirect

Polymer

journal homepage: www.elsevier.com/locate/polymer

Effects of molecular weight on poly(ω-pentadecalactone) mechanical and thermal properties

Jiali Cai [a], Chen Liu [a], Minmin Cai [a], Jie Zhu [b], Feng Zuo [b], Benjamin S. Hsiao [b,**], Richard A. Gross [a,*]

[a] NSF I/UCRC for Biocatalysis and Bioprocessing of Macromolecules, The Polytechnic Institute of New York University, Six Metrotech Center, Brooklyn, NY 11201, USA
[b] Department of Chemistry, Stony Brook University, Stony Brook, NY 11794, USA

ARTICLE INFO

Article history:
Received 17 November 2009
Received in revised form
4 January 2010
Accepted 7 January 2010
Available online 14 January 2010

Keywords:
Poly(ω-pentadecalactone)
Molecular weight
Tensile

ABSTRACT

A series of poly(ω-pentadecalactone) (PPDL) samples, synthesized by lipase catalysis, were prepared by systematic variation of reaction time and water content. These samples possessed weight-average molecular weights (M_w), determined by multi-angle laser light scattering (MALLS), from 2.5×10^4 to 48.1×10^4. Cold-drawing tensile tests at room temperature of PPDL samples with M_w between 4.5×10^4 and 8.1×10^4 showed a brittle-to-ductile transition. For PPDL with M_w of 8.1×10^4, inter-fibrillar slippage dominates during deformation until fracture. Increasing M_w above 18.9×10^4 resulted in enhanced entanglement network strength and strain-hardening. The high M_w samples also exhibited tough properties with elongation at break about 650% and tensile strength about 60.8 MPa, comparable to linear high density polyethylene (HDPE). Relationships among molecular weight, Young's modulus, stress, strain at yield, melting and crystallization enthalpy (by differential scanning calorimetry, DSC) and crystallinity (from wide-angle X-ray diffraction, WAXD) were correlated for PPDL samples. Similarities and differences of linear HDPE and PPDL molecular weight dependence on their mechanical and thermal properties were also compared.

1. Introduction

Polyethylene is the most widely used commodity polymer. It is found in many consumer products, such as milk jugs, detergent bottles, margarine tubs, garbage containers, water pipes, just to name a few. Poly(ω-pentadecalactone) (PPDL) is a new type of thermoplastic that can be synthesized by lipase catalysis [1–3]. The chemical structure of PPDL, with 14 methylene groups and an in-chain ester linkage in each repeating unit, is very similar to that of linear high density polyethylene (HDPE) (Scheme 1). Polyethylene (PE) cannot be easily decomposed into small molecules after usage. To achieve extensive degradation of the PE carbon backbone, treatment of PE with strong oxidized agents such as nitric acid [4], ozone [5] and permanganic acid [6] or pyrolysis at high reaction temperatures (above 370 °C) [7,8] is required. Therefore, "white pollution" [9,10] from un-recycled PE plastics is a mounting problem that mankind must confront. An important advantage of PPDL over PE is that the former has ester groups in the backbone that are susceptive to chain breakage. Consequently, gentle enzymatic hydrolysis can, in principle, be used to decompose PPDL back into monomer building blocks. Currently, on-going studies are in progress to find a suitable enzyme for PPDL biological recycling both in our laboratory and elsewhere [11].

Chemical catalysts such as potassium alkoxides [12], diethylzinc [13,14] and yttrium isopropoxide [15] can be used for conversion of macrolactones to polyesters. For ω-pentadecalactone (PDL), the use of immobilized lipase catalysis has been proven to be superior to chemical catalyzed routes for making polymers, resulting in more rapid polymerization kinetics as well as yielding polyesters of relatively higher molecular weight. Immobilized lipase-catalyzed polymerization of macrolactones was first published by Uyama et al. [16]. Our laboratory demonstrated that, using Novozym 435 that consists of *Candida antarctica lipase B* (CALB) physically immobilized on a macroporous support, the polymerization process of PDL gives PPDL with number-average molecular weight (M_n) up to 8.6×10^4 in yields exceeding 90% (route is illustrated in Scheme 1) [17]. Thus, enzyme-catalyzed preparation of PPDL with high molecular weight has provided suitable materials for evaluation of their physico-mechanical properties. For example, mechanical properties of PPDL with M_n 6.5×10^4 (polydispersity, M_w/M_n, 2.0) [18] and thiol-functionalized PPDL telechelics [19] have been studied.

Previous crystallographic work [20] indicated that the *a* and *b* parameters of PPDL unit cells are slightly larger than those of PE's

* Corresponding author. Tel.: +1 718 260 3408; fax: +1 718 260 3075.
** Corresponding author.
E-mail address: jlcai2004@yahoo.com (R.A. Gross).

0032-3861/$ – see front matter © 2010 Elsevier Ltd. All rights reserved.
doi:10.1016/j.polymer.2010.01.007

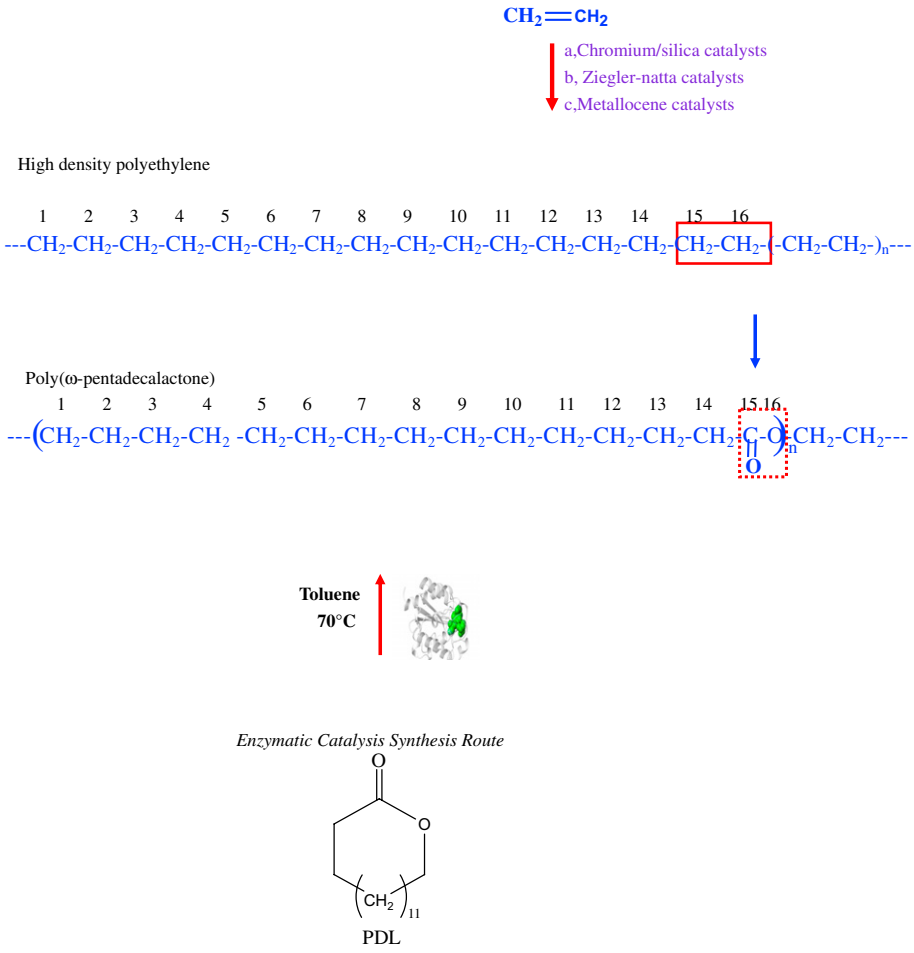

Scheme 1. Comparison of molecular structures of high density polyethylene (HDPE) and poly(ω-pentadecalactone) obtained via enzyme-catalyzed ring-opening polymerizations.

and the until cell parameter along the fiber axis is much larger than that of PE's. DMA tests showed that PPDL with M_n 6.5×10^4 had a glass transition at −27 °C. Also, the observed high storage modulus was attributed to high crystallinity as determined by DSC and WAXS [18]. PPDL-based copolymers with other monomers including trimethylene carbonate [2], *p*-dioxanone [3] and ω-caprolactone [21] were synthesized and studied by thermal and X-ray analysis. Copolymers were found to be highly crystalline random copolymers over the entire composition range. This behavior was attributed to co-crystallization of comonomer units in a common lattice or isomorphic substitution of comonomer units.

The current study aimed to investigate the effect of PPDL molecular weight on its mechanical, thermal and rheological properties. The chosen synthetic methods enabled the preparation of PPDL with M_w values up to 48.1×10^4 and PDI values close to 2.0. Films were prepared by press-molding at 130 °C and tensile testing was performed on these samples. Based on the shape of stress–strain curves, a brittle-to-ductile transition along with maximum elongation at break was observed. Since the chemical structure of PPDL is similar to polyethylene (PE), its thermal and mechanical properties were compared with those of a commercially obtained PE sample [22]. In addition, PPDL films with different molecular weights were analyzed by differential scanning calorimetry (DSC), wide-angle X-ray diffraction (WAXD), small-angle X-ray scattering (SAXS) and dynamic mechanical analysis (DMA) to reveal the molecular weight dependence of mechanical, thermal, crystalline and rheological properties. It was found that Young's modulus and stress at break exhibit distinct crystallinity dependence; in addition, differences, of elongation at break and true stress at break, between PPDL and linear PE, are discussed.

2. Experimental

2.1. Materials

Samples of ω-pentadecalactone (PDL, 98%) and anhydrous *p*-xylene (>99%) were purchased from Aldrich Chemical Co. and were used as received. Chloroform was purchased from PHARMCO-AAPER Inc. (>99.9%). Anhydrous toluene (98%), purchased from Aldrich Chemical Co., was dried over sodium and then was distilled under nitrogen. Novozym 435 (specific activity 10,000 PLU/g) was a gift from Novozymes (Bagsvaerd, Denmark) and consists of *Candida antarctica* Lipase B (CALB) physically adsorbed within the macroporous resin Lewatit VPOC 1600 (poly[methyl methacrylateco-butyl methacrylate], supplied by Bayer).

2.2. Sample preparation

2.2.1. Enzyme-catalyzed synthesis of PPDL samples 1–3 (Table 1)

Pentadecalactone (PDL, 40 g) was polymerized to prepare PPDL samples 1–3 at 70 °C, with magnetic stirring, in toluene (monomer:toluene = 1:2 wt/v), using Novozym 435 as the catalyst for predetermined reaction times (see Table 1). Reactions were carried out in 500 mL round-bottom flasks fitted with a magnetic stirrer and an inlet/outlet for nitrogen gas. No precautions were taken to dry the monomer, catalyst, solvent or glassware. The ratio of

Table 1
PPDL M_w and PDI values for PPDL samples and corresponding reaction times for sample synthesis.

Sample number	$M_w \times 10^{-4}$ [a]	PDI[b]	Reaction time (h)
1	2.5	4.9	6
2	4.5	3.3	13
3	8.1	3.1	24
4	18.9	1.6	8
5	28.0	2.0[c]	16
6	48.1	1.8	26

[a] From light scattering.
[b] PDI is polydispersity index that was determined by GPC relative to polystyrene.
[c] Calculation performed without inclusion of low molecular weight peaks observed in the GPC chromatogram (see Fig. 7).

Novozym 435 to PDL was 1% (w/w). All liquid transfers were performed by syringe through rubber septum caps under nitrogen. The final product mixture was dissolved in cold chloroform, filtered to remove catalyst beads, precipitated in methanol to remove unreacted PDL and then solvent was removed at 50 °C under vacuum for 16 h.

2.2.2. Enzyme-catalyzed synthesis of PPDL samples 4–6 (Table 1)

The method used was a variation of that described by de Geus [23] to obtain PPDL of higher molecular weight. PDL (50 g) was polymerized to prepare PPDL samples 4–6 in toluene (monomer:-toluene = 1:2 w/v), using Novozym 435 as the catalyst for predetermined reaction times (see Table 1). Reactions were conducted in 500 mL three-neck round-bottom flasks fitted with a glass overhead stirrer and connected to nitrogen and vacuum lines via a fire stone valve. The ratio of Novozym 435 to PDL was 1% (w/w). Vacuum pressure in the system was controlled (±0.2 mmHg) by a J-KEM vacuum regulator. Novozym 435 was dried for 16 h at 50 °C under 2 mmHg. The reaction vessel containing 3 Å sieves was predried at 150 °C (ambient pressure) for 16 h and, thereafter, was flame dried and the atmosphere was switched to dry nitrogen prior to monomer and solvent addition. Glass syringes and needles were pre-dried at 150 °C for 16 h and were cooled under a nitrogen purge till they was sufficiently cool to be handled for solvent and monomer transfers. Dry toluene (80 g) PDL (40 g) was added to the flask by syringe under nitrogen. Then, one port on the vessel was opened while purging with nitrogen and dried Novozym 435 was added. Reaction contents were heated by immersing the flask in an external oil bath at 85 °C. After the allotted reaction time, 150 mL of pre-heated *p*-xylene (100 °C) was added to the highly viscous slurry of enzyme, PPDL and toluene. The slurry was stirred for 1 h to dissolve PPDL and then filtered using a pre-heated Buchner-funnel. Small aliquots of pre-heated (100 °C) *p*-xylene solvent were used to quantitatively transfer reaction products. The filtrate was added slowly to cold methanol (200 mL) to precipitate PPDL that was collected using a Buchner-funnel. Finally, the polymer was dried under vacuum (2 mmHg) for 16 h at 50 °C to remove solvents.

2.3. Nuclear magnetic resonance characterization

Both ^{1}H and ^{13}C NMR spectra were recorded at room temperature on a DPX300 spectrometer (Bruker Instruments, Inc.) at 300 MHz in chloroform-*d*. Chemical shifts (in parts per million) for ^{1}H and ^{13}C NMR spectra were referenced relative to tetramethylsilane as an internal reference at 0.00. All synthesized PPDL materials described herein had identical NMR spectra with signals and assignments as follows: $-[C(=O)-CH_2^b-CH_2^c-(CH_2^d-CH_2^d-)_5-CH_2^c-CH_2^a-O]-$ ^{1}H NMR ($CDCl_3$, δ): 4.01 (t, *J* 6.5 Hz, CH_2^aO); 3.58 (t, *J* 6.5 Hz, CH_2OH); 2.24 (t, *J* 7.5 Hz, CH_2^bCO); 1.59, 1.22 (brs, $CH_2^{c,d}$) ppm. ^{13}C NMR ($CDCl_3$, δ): 173.9 ($COCH_2$), 64.4(CH_2^aO), 34.4($OCOCH_2^b$), 29.6–29.1, 28.6, 25.9, 25.0 (all other carbons) ppm.

2.4. Molecular weight determination

To determine the absolute molecular weight of PPDL samples, a Wyatt HELLOS multi-angle light scattering detector and a Wyatt Optilab rEx differential refractive index detector were used. These two detectors were connected by a steel tube with inner diameter 0.5 mm and a CRZEL syringe pump. The solution concentration ranged from 5×10^{-4} to 5×10^{-3} g/mL. Astra V software was used to acquire and process the data according to Zimm plots.

The relative molecular weight of PPDL samples were determined by gel permeation chromatography (GPC) using a Waters HPLC system equipped with a model 510 pump, model 717 autosampler, and model 410 refractive index detector with 500, 10^3, 10^4, and 10^5 Å Ultrastyragel columns in series. Waters Empower GPC software (Version 3, Viscotek Corp.) was used for data analysis. Chloroform was used as eluent at a flow rate of 1.0 mL/min. Sample concentrations and injection volumes were 0.2% w/v and 100 μL, respectively. The number-average molecular weight (M_n) and weight-average molecular weight (M_w) were determined based on a calibration curve generated by narrow molecular weight polystyrene standards (Aldrich Chemical Co). GPC and light scattering determined values of M_w were similar (within 12%). For PPDL molecular weight values reported herein, light scattering M_w and GPC M_w/M_n values were used (see Table 1).

2.5. Fractionation of PPDL sample 5

To separate low molecular weight material in sample 5, corresponding to GPC peaks observed at longer retention times, the sample was fractionated as follows. A solution containing 20 mL of chloroform and 0.2 g of Sample 5 was prepared. The mixture was maintained at 20 °C for 24 h with continual mixing by magnetic stirring. The 'insoluble' PPDL fraction was separated by filtration and solvent was removed in a vacuum oven at 40 °C for 7 days, giving 0.17 g of 'insoluble' solid sample. Solvent removal from the 'soluble' PPDL fraction was carried out by rotor-evaporation and subsequent drying in a vacuum oven, where the recovered 'soluble' PPDL sample was 0.03 g.

2.6. Tensile testing

Dumbbell shaped sample bars with dimensions of 20.0 mm (length) × 4.0 mm (neck width) × 1.5 mm (thickness) were prepared by press-molding at 130 °C and subsequent quenching at ambient temperature. An Instron 5542 tensile testing machine with a 500 N load cell was used for mechanical study (the crosshead speed was 3 mm/min and the test temperature was 25 °C). The Merlin software was used to collect and analyze the tensile results (stress was calculated according to the initial cross-section area). The values of tensile strength, Young's modulus, elongation at yield and break, stress at yield were obtained by averaging the data obtained from more than 4 specimens.

2.7. Dynamic mechanical analysis (DMA)

PPDL samples were molded into rectangular bars with dimensions of 30 mm (length) × 5 mm (width) × 1.5 mm (thickness). DMA measurements were performed in single-cantilever bending mode using a dynamic mechanical thermal analyzer (DMTA) (Tritec 2000 DMA, Triton Technology Company). Measurements were performed from 30 °C to 95 °C at a heating rate of 2 °C/min and frequency of 1 Hz. Two identical specimens with the same molecular weight were evaluated and results reported were mean values. The Triton Technology DMA Software was used to acquire and process the data.

2.8. Differential scanning calorimetry

DSC measurements were performed using a differential scanning calorimeter (Model 2920, TA Instruments). Temperature calibration was carried out using an indium standard. Measurements were performed under a nitrogen atmosphere at a flow rate of 50 mL/min. Typical parameters for experimental measurements are as follows: *i*) sample cooled to 10 °C, *ii*) heated to 150 °C at 10 °C/min, *iii*) held at 150 °C for 3 min and then *iv*) cooled to 10 °C at 10 °C/min. When temperature reached 10 °C, the sample was heated again to 200 °C at 10 °C/min. The melting temperature, melting enthalpy, crystallization peak temperature, and crystallization enthalpy were analyzed by using the TA Universal Analysis software.

2.9. X-ray measurements

Wide-angle X-ray diffraction (WAXD) and small-angle X-ray scattering (SAXS) experiments using the dumbbell shaped bars for tensile testing were carried out at the X27C beam line at the National Synchrotron Light Source (NSLS), Brookhaven National Laboratory (BNL). The wavelength of synchrotron radiation was 1.371 Å. A three-pinhole collimation system was used to reduce beam size to 0.6 mm in diameter. Two-dimensional (2D) WAXD and SAXS patterns were collected using a MAR CCD X-ray detector (MAR-USA), which had a resolution of 1024×1024 pixels (pixel size = 158.44 μm). The typical image acquisition time was 30 s for each data frame. Sample-to-detector distance was 1923.7 mm for SAXS (calibrated by a silver behenate, AgBe, standard) and 116.4 mm for WAXD (calibrated by an aluminum oxide, Al_2O_3, standard). All X-ray images were corrected for background scattering, air scattering and beam fluctuations. The obtained 2D SAXS and WAXD patterns were analyzed using the POLAR software to obtain one-dimensional SAXS and WAXD profiles. One-dimensional WAXD profiles were then processed by the linear square method to obtain crystallinity.

3. Results

3.1. PPDL synthesis

Previous work by our laboratory demonstrated that polymerization of PDL for 2 h at 70 °C in dry toluene (PDL to toluene 1:2 wt/vol) with 10 w/w-% monomer-to-catalyst gave PPDL (without fractionation) with M_n 7900 g/mol (GPC relative to polystyrene) [17]. Preparation of PPDL with higher molecular weights requires increasing diffusion constraints that slow chain propagation and decreasing reaction water content to start fewer chains [21,24–26]. To prepare a series of PPDL samples (1–3, Table 1) with relatively low molecular weight, the reaction temperature was maintained at 70 °C. Furthermore pre-drying of the reaction flask, enzyme and solvent was not carried out, while mixing was performed by magnetic stirring. After 1 h of reaction, the viscosity of the reaction mixture was sufficiently high which stopped magnetic stirring. Hence, the diffusion monomer in the reaction system became slow, which hindered the increase of molecular weight [17]. The molecular weight of the product within the series of samples 1–3 was only varied by the reaction time. By increasing the reaction time from 6 to 13 and 24 h, M_w of PPDL after precipitation increased from 2.5 to 4.5 and 8.1×10^{-4} g/mol (determined by light scattering, see Experimental Section), respectively.

Higher molecular weight PPDL samples 4, 5 and 6 were prepared by increasing the reaction temperature to 85 °C and using an overhead stirrer, both with the intent of increasing diffusivity of reactants. In addition, the reaction flask, syringes for reactant transfer, PDL, toluene and Novozym 435 were all dried prior to reactions (see Experimental Section). By increasing the reaction time from 8 to 16 and 26, samples 4, 5 and 6 were prepared having M_w values ($\times 10^{-4}$, determined by light scattering) of 18.8, 28.0 and 48.1 g/mol, respectively. For the above, PPDL was synthesized in quantities up to 40 g and yields from 75 to 80% after precipitation.

3.2. Tensile testing

Dumbbell shaped sample bars were prepared (see Experimental Section, above) for tensile testing. Sample 1 (M_w 2.5×10^4) was found to be too brittle to be tested. Stress–strain curves for Samples 2–6 are illustrated in Fig. 1(a–e). Fig. 1f displays four regions according to slope change in the stress–strain curve. Manson et al. [27] assigned these four regions as: I – linear and nonlinear viscoelasticity, II – neck region/strain softening, III – plastic flow, and IV – strain-hardening. The Young's modulus was determined as the slope of stress–strain curve at strain below 1% using the linear least square method. The values of strain and stress at yield were the (x, y) coordinates at which the first derivative of the stress–strain curve was zero. Values of elongation and stress at break represented the (x, y) coordinates after which the slope of the stress–strain curve became negative. The averaged results from replicated experiments are summarized in Table 2. Inspection of PPDL samples before stretching and after fracture showed that the volume of the bar subjected to high strain was found to be about two times that of the original volume (i.e. 50% polymer and 50% void formations). This observation is in agreement with that by Ward [28]. Since the stress value in Fig. 1 was estimated by the load divided by the initial cross-sectional area, for samples 4, 5, and 6, the true stress values at break were recalculated using the value of stress at break (in Fig. 1) multiplied by a factor (1 + strain)/2. For samples at lower strains (samples 2, 3), the true stress values at break were recalculated by the value of stress at break multiplied by a factor (1 + strain), i.e., neglecting the effect of volume increase at lower strains. The recalculated values of true stress at break are listed in Table 2. Variations of Young's modulus, true stress at break, elongation at break, and strain and stress at yield as a function of PPDL molecular weight are shown in Fig. 2(a–e).

The properties shown in Figs. 1 and 2 and Table 2 reveal unambiguously that they are dependent on PPDL molecular weight. Fig. 1a illustrates that, for sample 2 ($M_w = 4.5 \times 10^4$), stress first increased rapidly with strain but then the slope of stress–strain curve began to decrease. When strain reached 4.5 ± 0.8%, the sample fractured (the fracture was homogeneous as is typical for brittle fracture), while no neck was observed before fracture. As M_w increased to 8.1×10^4, the shape of the stress–strain curve (Fig. 1b) deviated substantially from that of sample 2. For sample 3, necking and plastic flow were observed during stretching; stress first reached the maximum value and then decreased, followed by stable propagation before fracture. When the sample bar length reached 237 ± 25% of the initial length, the sample bar fractured. Thus, with an increase in the molecular weight of about 2 times from sample 2 to sample 3, the elongation at break increases almost 30 times and the fracture fashion of PPDL changes from brittle-to-ductile. In addition, a stress-whitening phenomenon was observed during stretching of sample 3, which is quite different from sample 2. Interestingly, for PPDL of $M_w = 18.9 \times 10^4$ (sample 4), the elongation at break increased to 650 ± 30% while the strain-hardening phenomenon was also observed (Fig. 1c). With further increases in M_w, samples exhibited a similar stress–strain curve shape as that of sample 4 and values of elongation at break remained almost constant (e.g. 700 ± 70% for $M_w = 28 \times 10^4$ and 580 ± 30% for $M_w = 48.1 \times 10^4$). This suggests that for PPDL, it is not necessary to synthesize polymers with molecular weights above $M_w = 18.9 \times 10^4$ to attain higher draw

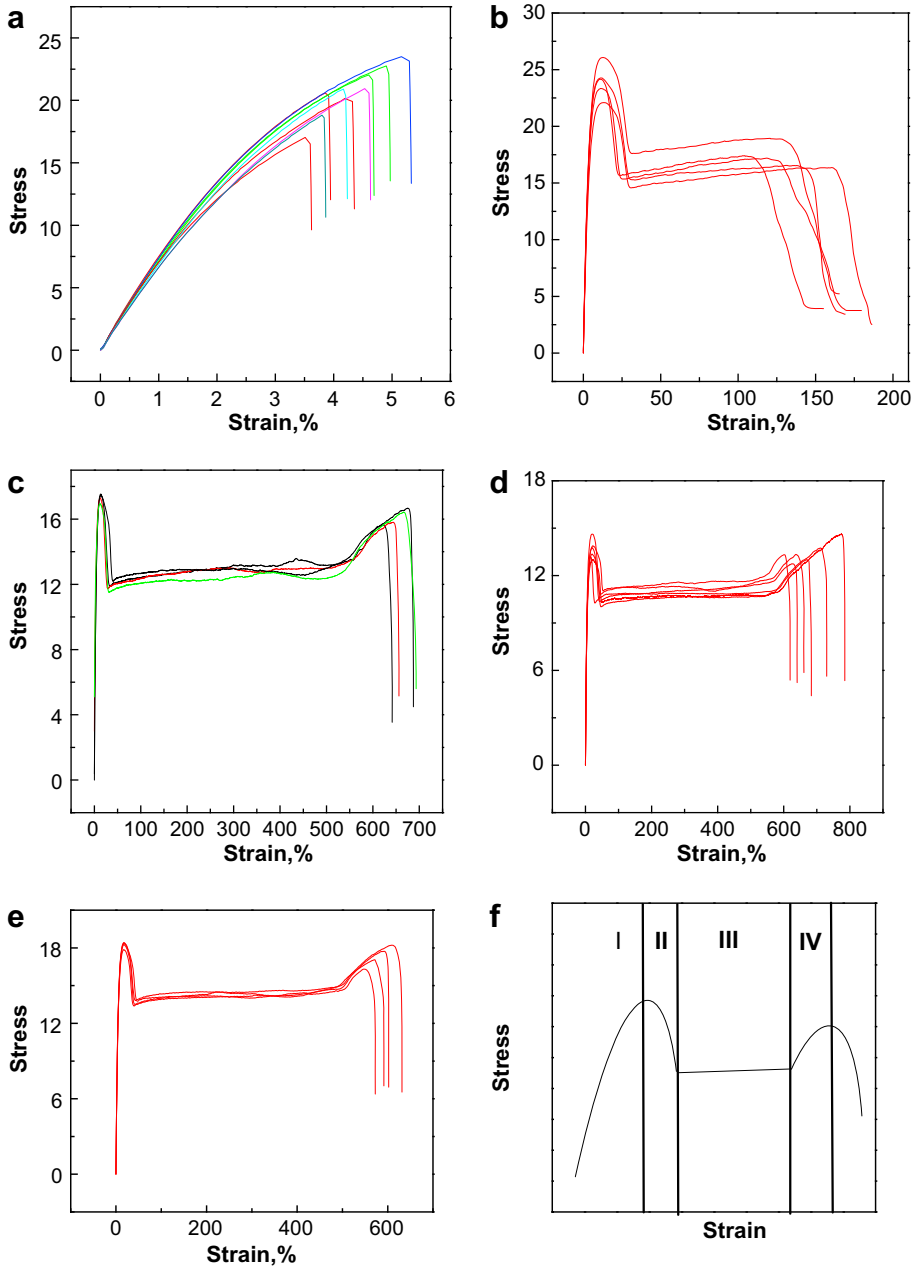

Fig. 1. Stress–strain curves for PPDLs with different molecular weights (a,2; b,3; c,4; d,5; e,6). Scheme f shows regions within the stress–strain curve of PPDL samples undergoing stretching. For each sample, repeated stress–strain measurements on fresh PPDL samples are plotted.

ratios since the elongation at break remains almost constant above $M_w = 18.9 \times 10^4$.

The plot of true stress at break (tensile strength) versus M_w (Fig. 2b) showed a similar trend as that of elongation at break versus M_w. The stress at break first increased from 21.3 MPa to 60.8 MPa as M_w increased from 4.5×10^4 to 18.9×10^4 and then remained almost constant at high M_w. The curve of Young's modulus versus M_w (Fig. 2c) exhibited a minimum at $M_w = 28.0 \times 10^4$. Young's modulus first decreased from 690 MPa to 290 MPa with increasing M_w, and then increased to 390 MPa. However, the corresponding curve of strain at yield versus M_w first increased with M_w from 12.0 to 20% and then decreased slightly to 17.4%. The trend of stress at yield versus M_w is almost opposite to that of strain at yield versus M_w, since the stress first decreased from 24.1 to 13.3 MPa, and then increased to 18.2 MPa with increasing M_w.

3.3. Thermal analysis

Thermal analysis of several samples with different molecular weight was carried out after processing samples into dumbbell shaped bars prior to tensile testing. Fig. 3displays DSC curves from first heating (Fig. 3a), cooling (Fig. 3b) and second heating (Fig. 3c) scans of PPDL samples (1–6). The trend of peak melting temperature with M_w in heating is similar to that in cooling curves. Values of melting enthalpy (ME) and melting temperature (MT) during first and second heating scans, and values of crystallization enthalpy (CE) and crystallization peak temperature (CPT) during cooling scans are summarized in Table 3. Since the trends of change in MT and ME during the first heating scan are similar to those during the second heating scan, only values of ME and MT in first heating and values of CE and CPT in cooling are plotted in Fig. 4a,b.

Table 2
Young's modulus, correlation coefficient in obtaining young's modulus, elongation to break, stress at break, stress at yielding, and strain at yielding for PPDL samples of differing molecular weight.

Sample No.	M_w ($\times 10^{-4}$)	Young's Modulus (MPa)	Correlation coefficient	Elongation at break (%)	Stress at break (MPa)	Stress at yield (MPa)	Strain at yield (%)
2	4.5	690 ± 40	0.9995	4.5 ± 0.8	20.4 ± 3.2 (21.3 ± 3.3)[a]	–	–
3	8.1	620 ± 50	0.99934	137 ± 25	17.7 ± 1.3 (42.0 ± 3.0)	24.1 ± 2.0	12.0 ± 1.0
4	18.9	450 ± 20	0.99872	650 ± 28	16.2 ± 0.5 (60.8 ± 2.0)	17.2 ± 0.3	13.0 ± 1.0
5	28.0	290 ± 30	0.99865	703 ± 72	13.7 ± 1.0 (55.0 ± 4.0)	13.3 ± 1.3	20.6 ± 1.3
6	48.1	390 ± 10	0.9989	580 ± 30	17.3 ± 0.9 (58.8 ± 3.1)	18.2 ± 0.3	17.4 ± 0.4

[a] The true stress at break calculated after cross-section area correction.

Fig. 4a indicates that ME first increased from 134.0 J/g to 164.4 J/g and then decreased afterward with increasing M_w. When M_w was 28.0×10^4, ME reached a minimum value (101.6 J/g); when M_w was 48.1×10^4, ME climbed back up to 115.3 J/g. Similarly, MT first increased from 97 °C to 103.2 °C, and then decreased to 91.7 °C, and again increased to 99.4 °C with increase of M_w. Upon crystallization of PPDL during cooling, the changes of CE and CPT with M_w were similar to those of ME and MT (Fig. 4b). Generally, the value of CE was smaller than that of ME in the same sample, possibly due to recrystallization upon heating [29].

3.4. X-ray measurements

To compare DSC results, wide-angle X-ray diffraction (WAXD) experiments were performed on the same dumbbell shaped sample bars prior to tensile testing. Fractions of crystalline phases plotted in Fig. 5 were obtained by peak deconvolution of integrated WAXD profiles. The trend of crystallinity change with M_w was similar to the variation of ME and CE with M_w. To compare the DSC and X-ray results, the values of crystallization enthalpy from cooling (instead of the melting enthalpy) were used in order to eliminate the effect of recrystallization during DSC scanning. The equilibrium melting enthalpy of PPDL had been estimated to be 264 J/g and 233 J/g, respectively, by Wunderlich [29] and Lebedv et al. [30]. If 233 J/g was used to calculate crystallinity values from DSC results, calculated crystallinity values would be higher than those from WAXD for samples with M_w less than 44.0×10^4 while the results were reverse when M_w was above 44.0×10^4. If 264 J/g was used, the calculated crystallinity from DSC was slightly higher than that from WAXD for samples with M_w less than 18.9×10^4; however, the calculated crystallinity from DSC was substantially lower than that from WAXD when M_w was above 18.9×10^4. Considering that the crystallinity calculation from WAXD includes contributions of both crystalline and interphase regions, while crystallization enthalpy from DSC is only from the crystal formation, the crystallinity value estimated from WAXD should be higher than those from DSC if the latter does not involve recrystallization. Thus, the value of 264 J/g was used in this study for calculations of PPDL crystallinity from DSC.

3.5. Dynamic mechanical analysis (DMA)

DMA was used in previous work [18] to measure the glass transition (−27 °C) and the effect of water content on β and γ relaxations for PPDL with $M_n = 6.5 \times 10^4$. In this study, DMA was used to compare the storage modulus of PPDL with different M_w values in the temperature range from 30 °C to 95 °C. Since sample 1 was brittle, only samples 2–6 were subjected to DMA tests. Fig. 6a illustrates curves of storage modulus vs. temperature for PPDL samples with different molecular weights. For each sample, the storage modulus decreased with increasing temperature and no distinct transitions were observed. The results in samples 3 and 4 exhibited an intersection at 85 °C, while samples 5 and 6 exhibited an intersection at 56 °C. Storage moduli at 40–90 °C for five samples are listed in Table 4 and displayed in Fig. 6b. This figure indicates that the trend of storage modulus changes with M_w at 40 °C was similar to that of the Young's modulus with M_w (Fig. 2c). Interestingly, as the temperature increased from 40 to 60 °C, the discrepancy between samples 5 and 6 decreased. For temperatures above 60 °C, the storage moduli of samples 5 and 6 are the same. This implies that above 60 °C, the molecular networks formed for samples 5 and 6 have the same elastic rigidity.

4. Discussion

This section considers the effects of M_w on PPDL mechanical, thermal and crystallization properties and compares these to those of linear PE.

4.1. Effects of molecular weight on PPDL properties

The effect of molecular weight of linear HDPE on its tensile properties was studied by Ward et al. [22]. They reported that Young's modulus decreases with increasing M_w. Since PPDL has a similar chemical structure as linear PE, its M_w dependence of Young's modulus should show a similar trend. However, The results herein appear to be different from those reported by Ward et al. [22] For example, in Fig. 2c, Young's modulus first decreases to a minimum (at sample 5, M_w 28.0×10^{-4}) and then increases. Without sample 5, behavior of PPDL would be similar to linear PE. Perhaps this can be rationalized as follows. Several other studies have indicated that the degree of crystallinity is the primary factor affecting the Young's modulus of semi-crystalline polymers [31–34]. It was known that low M_w fractions can act as diluents and retard the crystallization of higher M_w fractions [29]. Furthermore, low M_w fractions usually contribute less to the Young's modulus due to the lower possibility to form entanglements or tie molecules to transmit the stress [34]. In sample 5, the GPC spectrum clearly exhibits several peaks corresponding to low M_w fractions (Fig. 7). These low M_w fractions would be expected to decrease crystallinity and lower the Young's modulus. To verify this hypothesis, the following experiment was performed. Sample 5 was first immersed

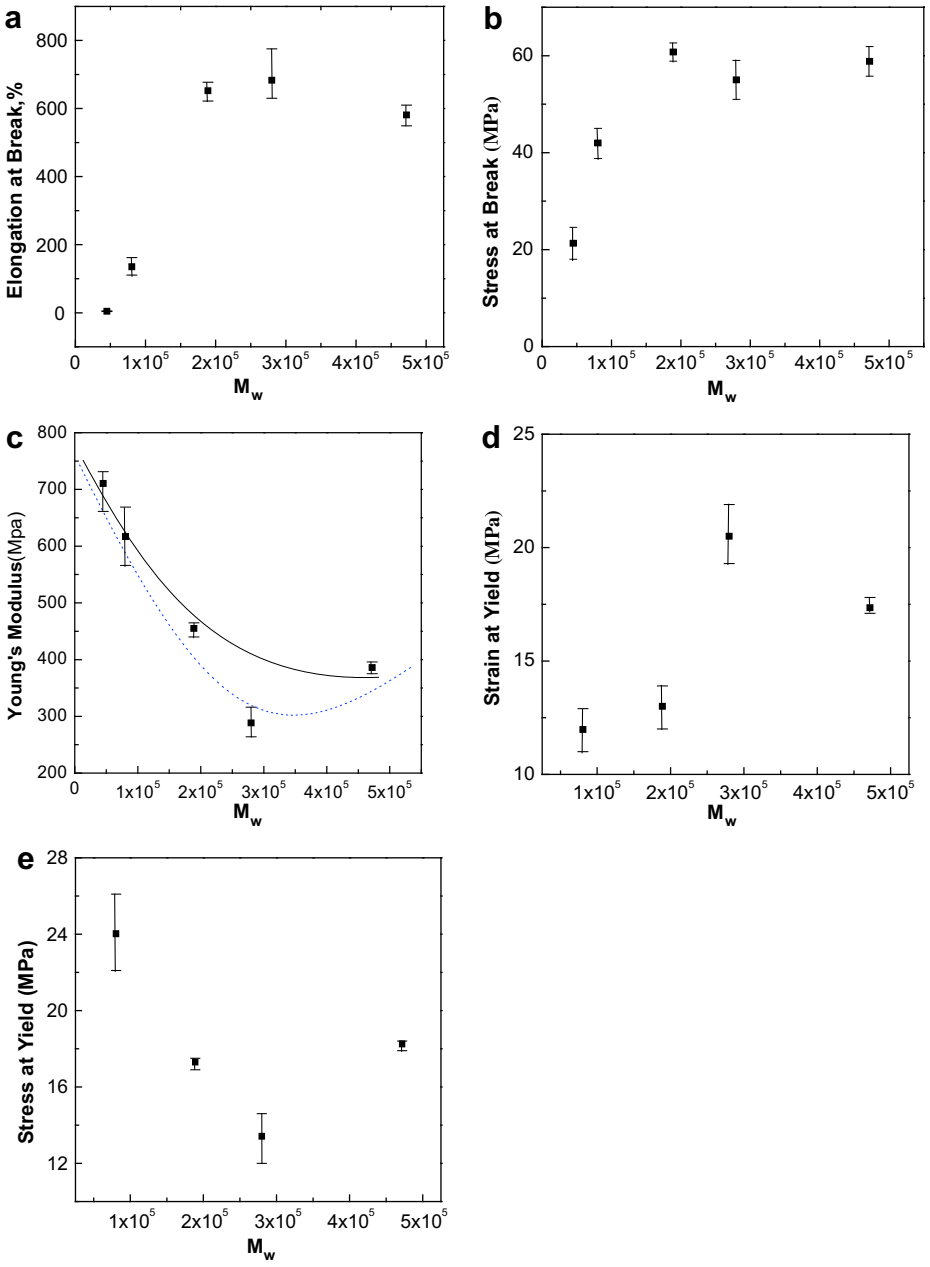

Fig. 2. Variations of as a function of PPDL molecular weight for tensile tests at 25 °C of: (a) elongation at break, (b) true stress at break, (c) young's modulus, (d) strain at yielding and (e) stress at yielding. The solid and dotted lines in c indicate how trends in Young's modulus as a function of molecular weight changes with and without sample 5, respectively.

in chloroform for 24 h at 20 °C to solubilize a large part of low M_w fractions. The remaining insoluble material after thorough removal of solvent was subjected to GPC and DSC analyses. The GPC chromatogram displayed in Fig. 7 indicates that a substantial part of low molecular weight fractions were removed by solubilization in chloroform. DSC results indicate that, after solvent extraction, the melting peak of sample 5 shifted to a higher temperature during both first and second heating scans (Fig. 8). The melting temperature, melting enthalpy for the first and second heating, the cooling crystallization peak, and cooling crystallization enthalpy are listed in Table 3 for comparison with data for non-fractionated sample 5. Indeed, the value of melting enthalpy increases after extraction and falls between those of samples 4 and 6. Thus, it appears that the crystallinity and Young's modulus of PPDL have a similar molecular weight dependence as linear PE based on studies by Ward et al. [28], i.e., both decrease with increasing M_w.

4.2. Young's modulus as a function of crystallinity

Since crystallinity plays a major role to influence Young's modulus, their relationship was investigated. The crystallinity was calculated by dividing the cooling crystallization enthalpy with the equilibrium enthalpy value of 264 J/g [29]. The relationships between crystallinity and Young's modulus are shown in Fig. 9a. The data set can be represented by a straight line without the extrapolation to the origin. This behavior was also observed by Mandelkern et al. [35], who measured the crystallinity of fractionated linear PE by density measurement. Flory and Yoon [35] pointed out that the initial chain topology in the molten polymer can be conserved during crystallization. In other words, the topological features such as entanglements, knots, loops and related structures can be regulated in the inter-lamellar amorphous region. Without question, these types of structures will affect the elastic

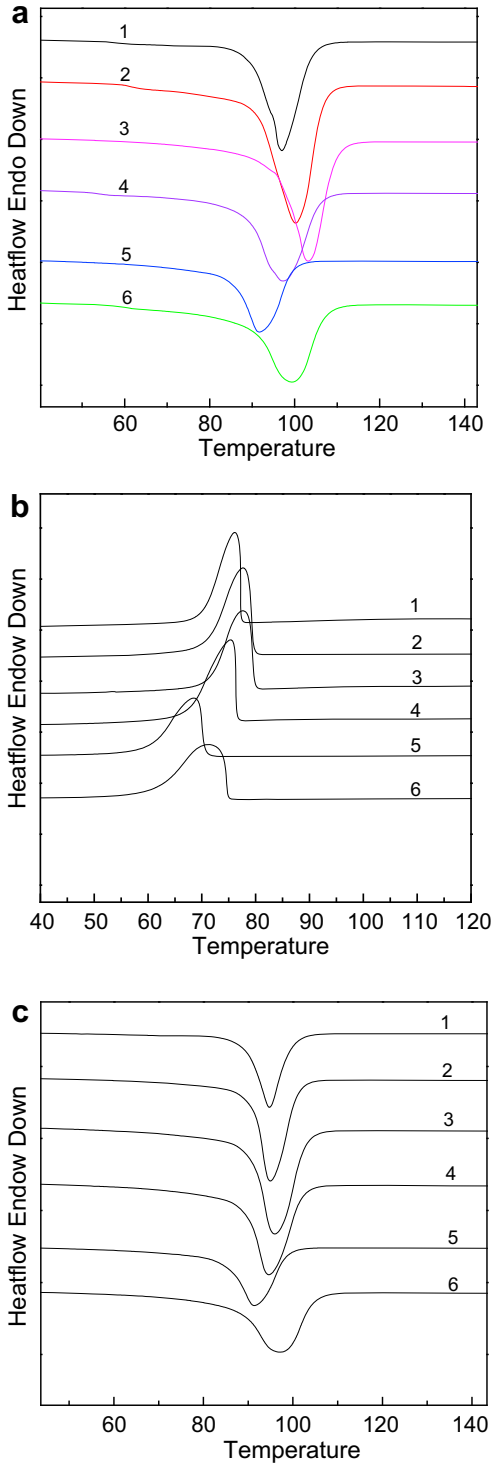

Fig. 3. DSC thermograms recorded for PPDL samples 1– 6 during: (a) first heating, (b) cooling and (c) second heating.

properties. In addition, the interphase region that connects the ordered crystalline region and the isotropic conformational disordered amorphous region can also contribute to elastic modulus [34]. A schematic diagram indicating different chain topologies in the lamellar structure of PPDLs with different M_w is shown in Fig. 10, which will be used to explain the different observed properties in the samples.

Table 3
DSC results of melting point (T_m), crystallization peak temperature (T_{cp}), melting enthalpy (ΔH_m), and cooling crystallization enthalpy (ΔH_c) for PPDL of differing M_w values.

$M_w \times 10^{-4}$	First heating		Second heating		Cooling	
	ΔH_m, J/g	T_m, °C	ΔH_m, J/g	T_m, °C	ΔH_c, J/g	T_{cP}, °C
2.5	134.0	97.0	131.4	94.7	134.1	76.1
4.5	164.4	100.2	151.0	95.0	141.1	77.7
8.1	147.3	103.2	143.1	96.0	135.6	77.6
18.9	120.7	97.2	128.4	94.6	118.0	75.4
28.0	101.6	91.7	99.3	91.4	92.2	68.5
	(118.6)[a]	(103.2)	(115.8)	(98.3)	(103.8)	(70.5)
48.1	115.3	99.4	110.1	97.1	97.7	71.2

[a] Samples extracted with chloroform for 24 h at 20 °C.

4.3. Yield stress as functions of crystallinity and crystallite thickness

The plot of yield stress versus crystallinity is shown in Fig. 9b, where the behavior can be rationalized by the occurrence of one or both of the following phenomena [36–38]. One possibility is a partial melting-recrystallization process is induced by deformation [36]. An alternative explanation is based on the screw dislocation theory [37,38]. The mechanism of deformation-induced

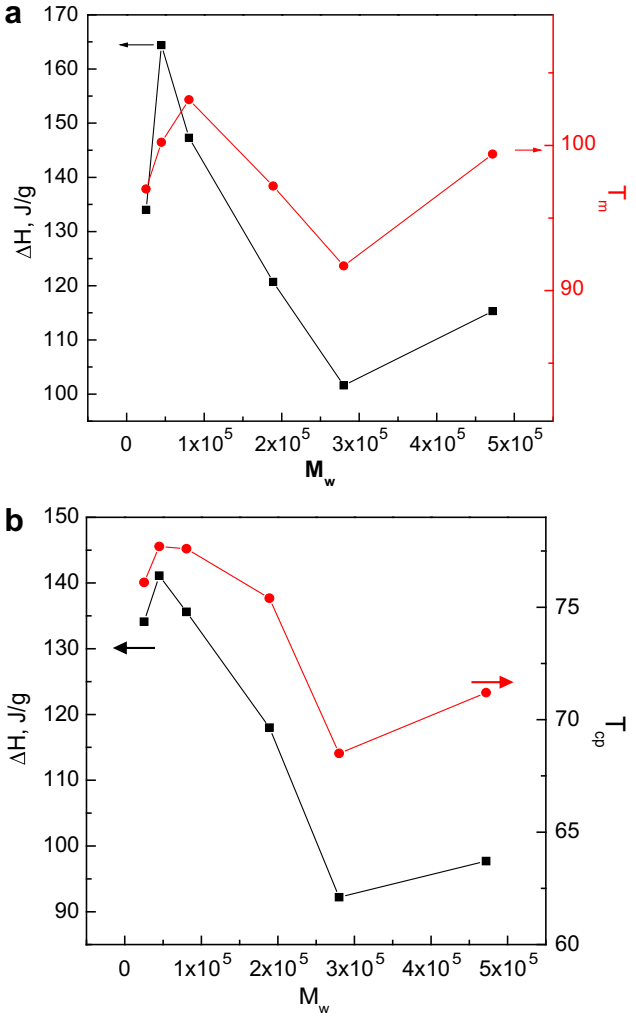

Fig. 4. Plots of melting enthalpy, melting point (T_m), crystallization enthalpy and crystallization peak temperature (T_{cp}) as a function of PPDL molecular weight recorded by DSC during: (a) first heating and (b) cooling.

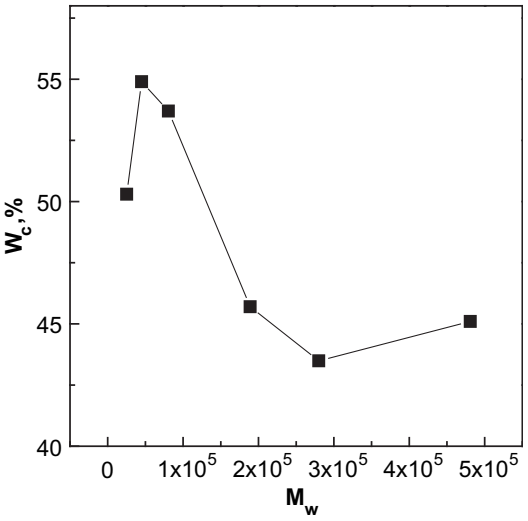

Fig. 5. Crystallinity of PPDL, determined by wide-angle X-ray diffraction (WAXD), as a function of PPDL molecular weight.

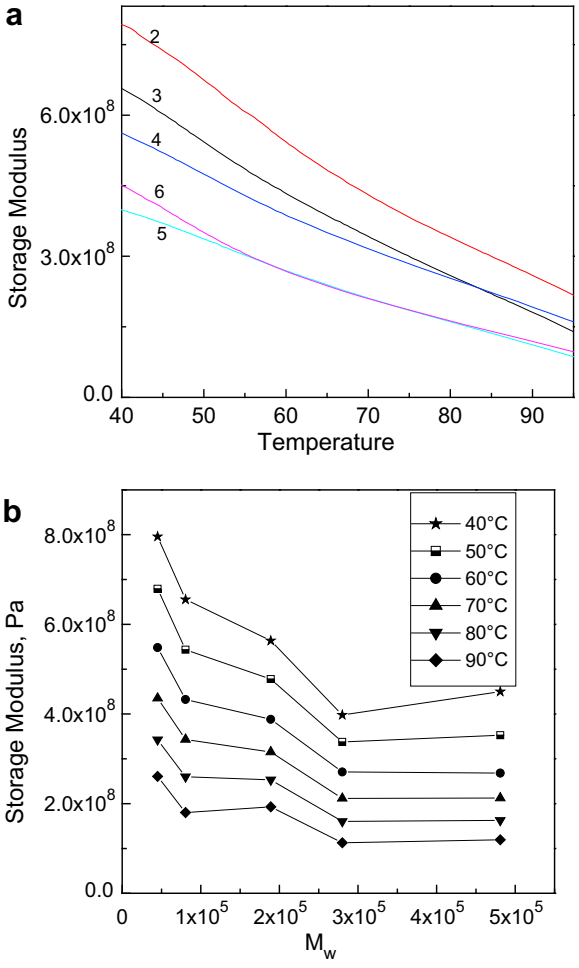

Fig. 6. (a) Plots of storage modulus as a function of temperature for PPDL with different molecular weight (2, $M_w = 45{,}000$; 3, $M_w = 81{,}000$; 4, $M_w = 189{,}000$; 5, $M_w = 280{,}000$; 6, $M_w = 481{,}000$); (b) dependence of storage modulus on PPDL molecular weight at selected temperatures.

Table 4
Storage modulus of PPDL samples of differing M_w at varying temperatures.

$M_w \times 10^{-4}$	Modulus, Pa					
	40 °C	50 °C	60 °C	70 °C	80 °C	90 °C
4.5	8.0×10^8	6.8×10^8	5.5×10^8	4.4×10^8	3.4×10^8	2.6×10^8
8.1	6.6×10^8	5.4×10^8	4.3×10^8	3.4×10^8	2.6×10^8	1.8×10^8
18.9	5.6×10^8	4.8×10^8	3.9×10^8	3.2×10^8	2.5×10^8	1.9×10^8
28.0	4.0×10^8	3.4×10^8	2.7×10^8	2.1×10^8	1.6×10^8	1.1×10^8
48.1	4.5×10^8	3.5×10^8	2.7×10^8	2.1×10^8	1.6×10^8	1.2×10^8

melting-recrystallization is based on previous experimental results by observation of transmission electron microscopy [39] and small-angle neutron scattering [40] results with linear PE. The screw dislocation theory argues that the shear yield stress (i.e., experimental yield stress/2) is related to the crystallite thickness by the following expression:

$$\tau_y = \frac{\kappa}{4\pi}\left[\exp\left(\frac{2\pi\Delta G_c}{\kappa b^2 L_c} + 1\right)\right]^{-1} \quad (1)$$

where τ_y is the shear yield stress, L_c is the crystal lamellar thickness, κ is a function of the crystal shear modulus, b is the Burgers vector having the same value as the PPDL unit cell c-axis, ΔG_c is the critical activation energy for dislocation growth, with values in the range between 40 and 80 κT. To correlate the relationship between yield stress and crystallite thickness, SAXS experiments were carried out where the results (the Lorentz-corrected SAXS profiles) are shown in Fig. 11. These profiles exhibit two peaks at very low q values. To obtain the long period L and crystallite thickness L_c, the one-dimensional correlation function $K(r)$ is calculated by the following equation [41]:

$$K(r) = \frac{1}{2\pi^2}\int_0^{\pi} Iq^2 \cos(qr)\mathrm{d}q \quad (2)$$

where $I(q)$ is the scattering intensity and r is the distance for which the electron density correlation is measured. The long periods for samples 3, 4, 5 and 6 were 17.5 nm, 18.9 nm, 19.3 nm and 18.1 nm, respectively. Assuming the crystal thickness should be thicker than the amorphous regions in the two-phase model, the estimated

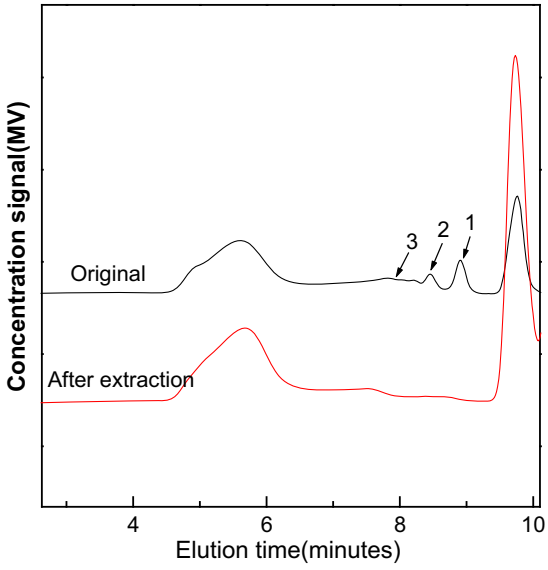

Fig. 7. Comparison of GPC curves for PPDL sample 5 before and after solvent extraction.

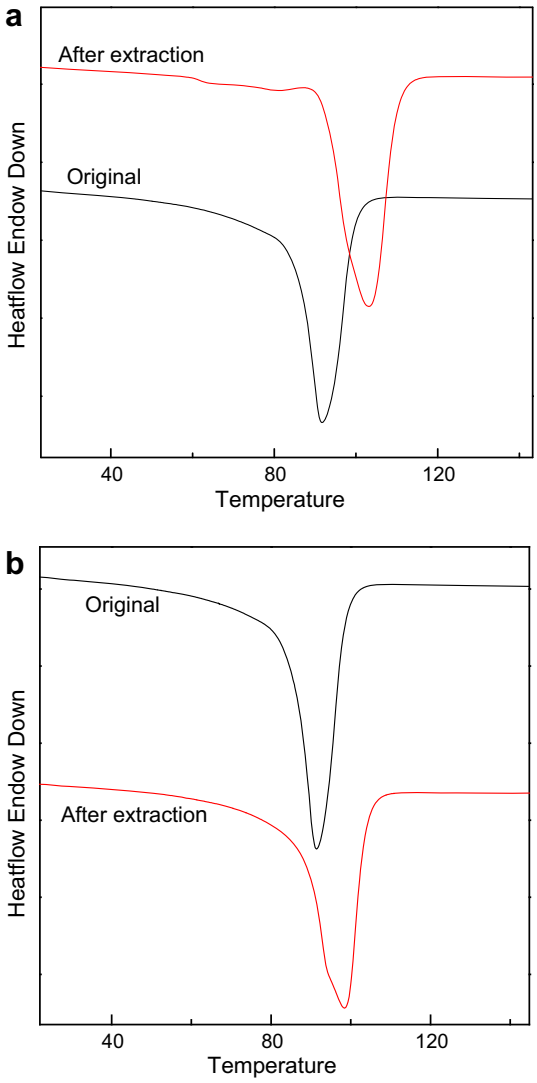

Fig. 8. Effect of sample fractionation melting of PPDL sample 5 determined by DSC thermograms during: (a) first heating and (b) second heating scans.

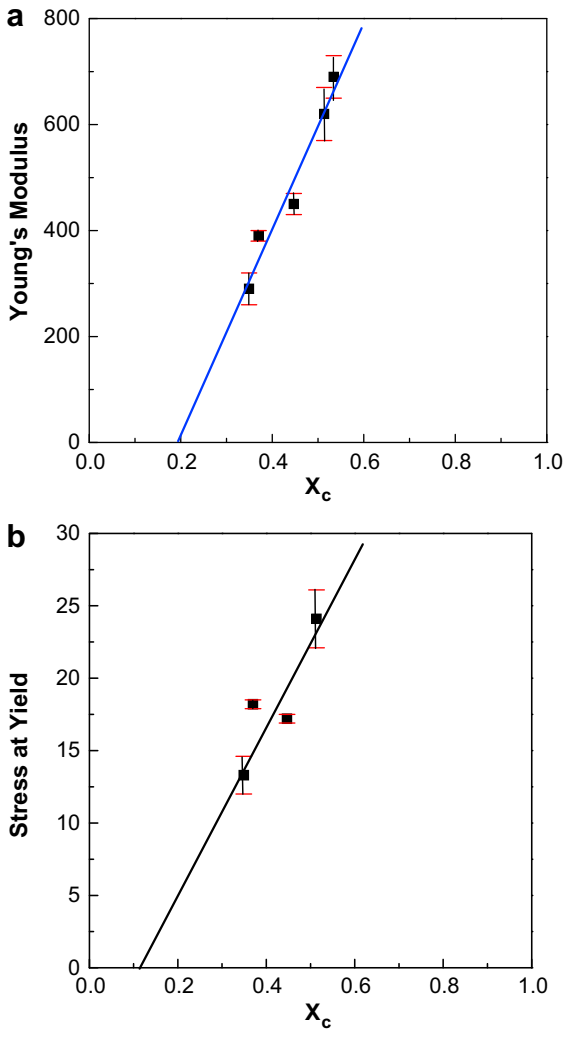

Fig. 9. Plots of Young's modulus (a) and stress at yield (b) as a function of PPDL crystallinity.

crystalline thickness values are 10.7 nm, 12.2 nm, 13.4 nm, 11.1 nm, respectively. The close values of the crystalline thickness lead us to conclude that the screw dislocation theory is not appropriate to explain yield stress data.

4.4. Strain and true stress at break

Several studies [22,35,42–45] have been reported dealing with the molecular weight effect on draw ratio for PE. The results indicate that the draw ratio decreases (e.g. 18–3) with increasing molecular weight of linear PE, whereas the true stress at break value exhibits a maximum at $M_w = 30.0 \times 10^4$ [33]. Results for PPDL samples are different from that obtained with PE. For PPDL, when M_w increases to 18.9×10^4, the draw ratio reaches an asymptotic value of about 7.5 (Fig. 2a). Interestingly, the corresponding true stress at break also reaches an asymptotic value of about 60.0 MPa at $M_w = 18.9 \times 10^4$ (Fig. 2b). One possible explanation for the discrepancy is as follows. Since the PPDL chain consists of C–C and C(=O)–O (or–O–C–) bonds along the backbone, where the C–C bond has larger bond energy than C(=O)–O (or –O–C–) bonds. Hence, the stress distribution should be heterogeneous along the chain during stretching. In high M_w samples ($>18.9 \times 10^4$),

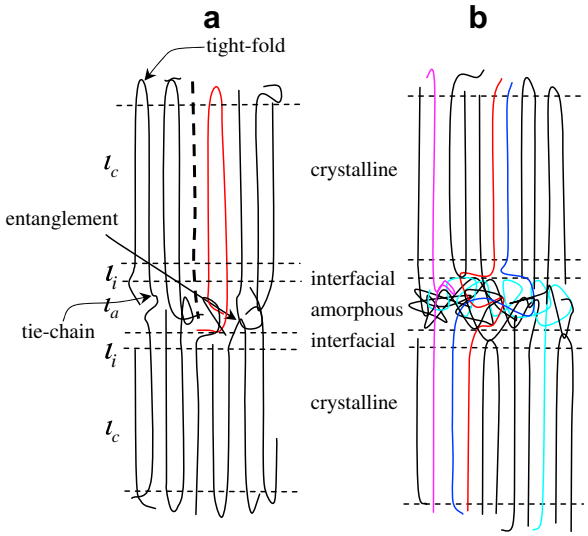

Fig. 10. Possible mechanism responsible for the brittle-to-ductile transition in: (a) lower molecular weight fraction and (b) higher molecular weight fraction.

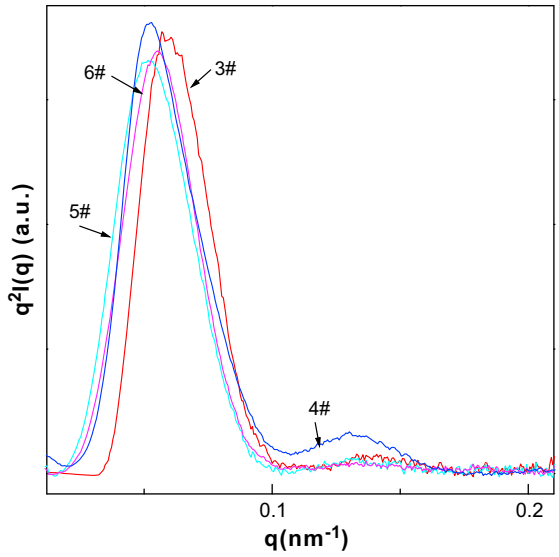

Fig. 11. Lorentz-corrected SAXS profiles of PPDL samples 3– 6 before stretching.

increased M_w would lead to enhanced strength of the entanglement network in the molten melt as well as in the inter-lamellar amorphous region when solidified. However, as the C–O bond is weaker than the C–C bond, the former probably breaks at a lower stress under deformation, thus limiting the ultimate strength of PPDL. This hypothesis is consistent with the observation of constant stress as well as the constant elongation at break value above $M_w = 18.9 \times 10^4$ under deformation. This may also explain why PE has a much higher draw ratio (18 or higher) than PPDL of the same or higher M_w, as the PE chain has only carbon–carbon bonds [32]. In general, variations of elongation and true stress at break (tensile strength) with M_w observed in this study are consistent with those reported in a tensile study of cellulose acetate by Sookne et al. [45] and the theoretical predication of Flory [46].

4.5. Brittle-to-ductile transition

The brittle-to-ductile transition in semi-crystalline polymers can be affected by many factors such as deformation rate and crystallinity [28,34]. Usually, increases in deformation rate and crystallinity will cause the brittle-to-ductile transition to shift towards higher M_w. However, molecular weight is still the most important factor that affects the material if the brittle-to-ductile transition is observed. Mandelkern et al. [35] found that for $M_w \leq 4.0 \times 10^4$, PE materials are brittle over the accessible range of crystallinities. When M_w is 7.0×10^4, the brittle-to-ductile transition can be observed. Furthermore, when the crystallinity is higher, the transition becomes sharper. In higher M_w PE (about 31.6×10^4) the brittle-to-ductile transition was not observed by increasing PE crystallinity. For PPDL, the M_w at which the brittle-to-ductile transition occurs (Fig. 2) is in agreement with the M_w range observed for PE. In addition, quenched PPDL sample 3 exhibited ductile behavior, while the annealed sample with higher crystallinity revealed brittle behavior. This finding agrees with Mandelkern's experiments on linear fractioned PE with $M_w = 7.0 \times 10^4$ [35].

Finally, we caution that when assessing the mechanical properties of PPDL samples of different molecular weights, in addition to crystallinity, crystallite thickness, inter-lamellar thickness and density of physical entanglements in the amorphous region, the fraction of the interfacial region and supermolecular morphology should also play an important role [34,47,48], which will be considered in our future studies.

5. Conclusions

Synthesis of large-scale PPDL samples was performed by lipase catalysis. Variation of PPDL M_w from 2.5 to 48.1×10^4 was achieved by manipulating reaction variables including reaction water content, method of mixing and reaction time. Tensile testing, DSC, X-ray, DMA and GPC were used to investigate the effect of molecular weight on mechanical, thermal and crystalline material properties. Cold-drawing tensile tests at room temperature revealed a brittle-to-ductile transition for PPDL samples with M_w values between 4.5×10^4 and 8.1×10^4. For PPDL with $M_w = 8.1 \times 10^4$, the entanglement network strength in non-crystalline regions is not sufficiently high to transmit stress during stretching, whereby interfibrillar slippage dominates until fracture. As PPDL M_w is increased from 18.9×10^4 and above, the entanglement network strength is greatly enhanced and strain-hardening takes place at high strains prior to failure. Furthermore, the elongation at break and tensile strength (i.e., true stress at break) reach asymptotic values of 650% and 60.8 MPa, respectively. The trends for changes in Young's modulus, melting enthalpy (from DSC) and crystallinity (from WAXD) as a function of molecular weight are all similar. Abnormality of one sample (5) was explained by its contamination with high levels of a lower molecular weight fraction. Storage modulus (from DMA) revealed similar molecular weight dependence trends at temperatures below 60 °C. However, above 60 °C, storage moduli of higher molecular weight samples becomes indistinguishable, indicating that the crystalline network structures of these samples at higher temperatures are also similar. Overall comparisons between PPDL and linear high density polyethylene (HDPE) mechanical properties showed similar trends in Young's modulus with molecular weight, but differing trends with respect to elongation at break and true stress at break as a function of molecular weight. The latter differences are explained by the presence of a low but persistent density of C–O bonds in ester links of PPDL that are not present in PE. We therefore conclude that PPDL-like polyesters have excellent potential to function in similar ways to PE. This bodes well to the potential further development of similar or related polymers for commercial use. Indeed, our laboratory has developed biocatalytic methods using an engineered *Candida tropicalis* strain to convert fatty acids, such as tetradecanoic acid, in volumetric yields of up to 160 g/L to their corresponding ω-hydroxyfatty acid (e.g. ω-hydroxytetradecanoic acid) (manuscript in review). Subsequent conversion of ω-hydroxyfatty acids to polyesters by condensation polymerization will provide a low-cost scalable route to biobased PPDL-like materials that can function in similar ways to PE.

Acknowledgements

The authors thank the National Science Foundation (NSF) and industrial members of NSF-I/UCRC for Biocatalysis and Bioprocessing of Macromolecules at NYU/Polytechnic University for financial support, intellectual input, and encouragement during the course of this research. BH also thanks support from NSF (DMR-0906512). We are also grateful to Mr. Seong Chan Park and Dr. Miriam Rafailovich at SUNY at Stony Brook for providing access to their Instron Tensile testing and DMA equipment.

References

[1] Mazzocchetti L, Scandola M, Jiang ZZ. Macromolecules 2009;42:7811.
[2] Ceccorulli G, Scandola M, Kumar A, Kalra B, Gross RA. Biomacromolecules 2005;6(2):902.
[3] Jiang ZZ, Azim HS, Gross RA, Focarete ML, Scandola M. Biomacromolecules 2007;8:2262.
[4] Keller A, Martuscelli E, Priest DJ, Udagawa Y. J Polym Sci Part A-2 1971;9:1807.

[5] Patel GN, Keller A. J Polym Sci Polym Phys Ed 1975;13(2):303.
[6] Haridoss S, Perlman MM. J Appl Phys 1984;55:1332.
[7] Sezgin A, Cha WS, Smith JM, Mccoyb J. Ind Eng Chem Res 1998;37(7):2582.
[8] Zhang JG, Jiang DD, Wilki CA. Polym Degrad Stab 2006;91(4):641.
[9] Fang CQ, Li TH, Zhang ZP, Jing DQ. Polym Comp 2008;29(5):500.
[10] <http://www.rrcap.unep.org/uneptg05/outline/env/white.pdf>.
[11] Meulen I, Geus M, Antheunis H, Deumens R, Joosten EAJ, Koning CE, et al. Biomacromolecules 2008;9:3404.
[12] Jedlinski Z, Juzwa M, Adamus G, Kowaczuk M. Macromol Chem Phys 1996;197:2923.
[13] Makovetsky KL. Vysokomol Soedin Ser B 1999;41(9):1525.
[14] Yevstropov A, Lebedev BV, Kiparisova Y. Vysokomol Soedin Ser A 1983;25:1679.
[15] Zhong Z, Dijkstra PJ, Feijen J. Macromol Chem Phys 2000;201:1329.
[16] Uyama H, Takeya K, Kobayashi S. Bull Chem Soc Jpn 1995;68:56.
[17] Kumar A, Kalra B, Dekhterman A, Gross RA. Macromolecules 2000;33:6303.
[18] Focarete ML, Scandola M, Kumar A, Gross RA. J Polym Sci Part B Polym Phys 2001;39:1721.
[19] Simpson N, Takwa M, Hult K, Johansson M, Martinelle M, Malmström E. Macromolecules 2008;41:3613.
[20] Gazzano M, Malta VA, Focarete ML, Scandola M, Gross RA. J Polym Sci Part B Polym Phys 2003;vol. 41:1009.
[21] Focarete ML, Gazzano M, Scandola M, Kumar A, Gross RA. Macromolecules 2002;35:8066.
[22] Capaccio G, Ward IM. Polymer 1975;16:239.
[23] Matthijs de Geus. Enzymatic catalysis in the synthesis of new polymer architectures and materials. Ph.D. thesis. Eindhoven University of Technology, Netherlands; Feb. 2007 [chapter 5].
[24] Kumar A, Gross RA. Biomacromolecules 2000;1:133.
[25] Bisht KS, Henderson LA, Gross RA, Dl Kaplan, Swift G. Macromolecules 1997;30(9):2705.
[26] Mei Y, Kumar A, Gross RA. Macromolecules 2002;35:5444.
[27] Manson JA, Hertzberg RW. CRC Crit Rev Macromol Sci 1973;1:433.
[28] Ward IM. Mechanical properties of solid polymers, vol. 399. John Wiley & Sons Pub; 1983 [chapter 12].
[29] Wunderlich B. Advanced thermal analysis. Databank of thermodynamic properties of linear macromolecules and small molecules. Knoxville, TN, USA: Department of Chemistry, University of Tennessee; 1995.
[30] Lebedev B, Yevstropov A. Makromol Chem 1984;185:1235.
[31] Keith HD, Paden FJ, Vadimsky RG. J Appl Phys 1971;42:4585.
[32] Capaccio G, Crompton TA, Ward IM. J Polym Sci Part B Polym Phys 1976;14:1641.
[33] Mandelkern L. Polym J 1985;17:337.
[34] Mandelkern L. Acc Chem Res 1990;23:380.
[35] Kennedy MA, Peacock AJ, Mandelkern L. Macromolecules 1994;27:5297.
[36] Flory PJ, Yoon DY. Nature 1978;272:226.
[37] Young RJ. Philos Mag 1974;30:85.
[38] Crist B, Fischer CJ, Howard PR. Macromolecules 1989;22:1709.
[39] Philips PJ, Philipot RJ. Polym Commun 1986;27:307.
[40] Wu W, Wignall GD, Mandelkern L. Polymer 1992;33:4137.
[41] Strobl GR, Schneider M. J Polym Sci Part B Polym Phys 1980;18:1343.
[42] Andrews JM, Ward I. J Mater Sci 1970;5:411.
[43] Williamson GR, Wright B, Haward RW. J Appl Chem 1964;14:131.
[44] Popli R, Mandlkern L. J Polym Sci Polym Phys Ed 1987;25:441.
[45] Sookne AM, Harris M. Ind Eng Chem 1945;37(5):478.
[46] Flory PJ. J Am Chem Soc 1945;67:2048.
[47] Peterlin A. J Mater Sci 1971;6:490.
[48] Vincent PI. Polymer 1960;1:425.